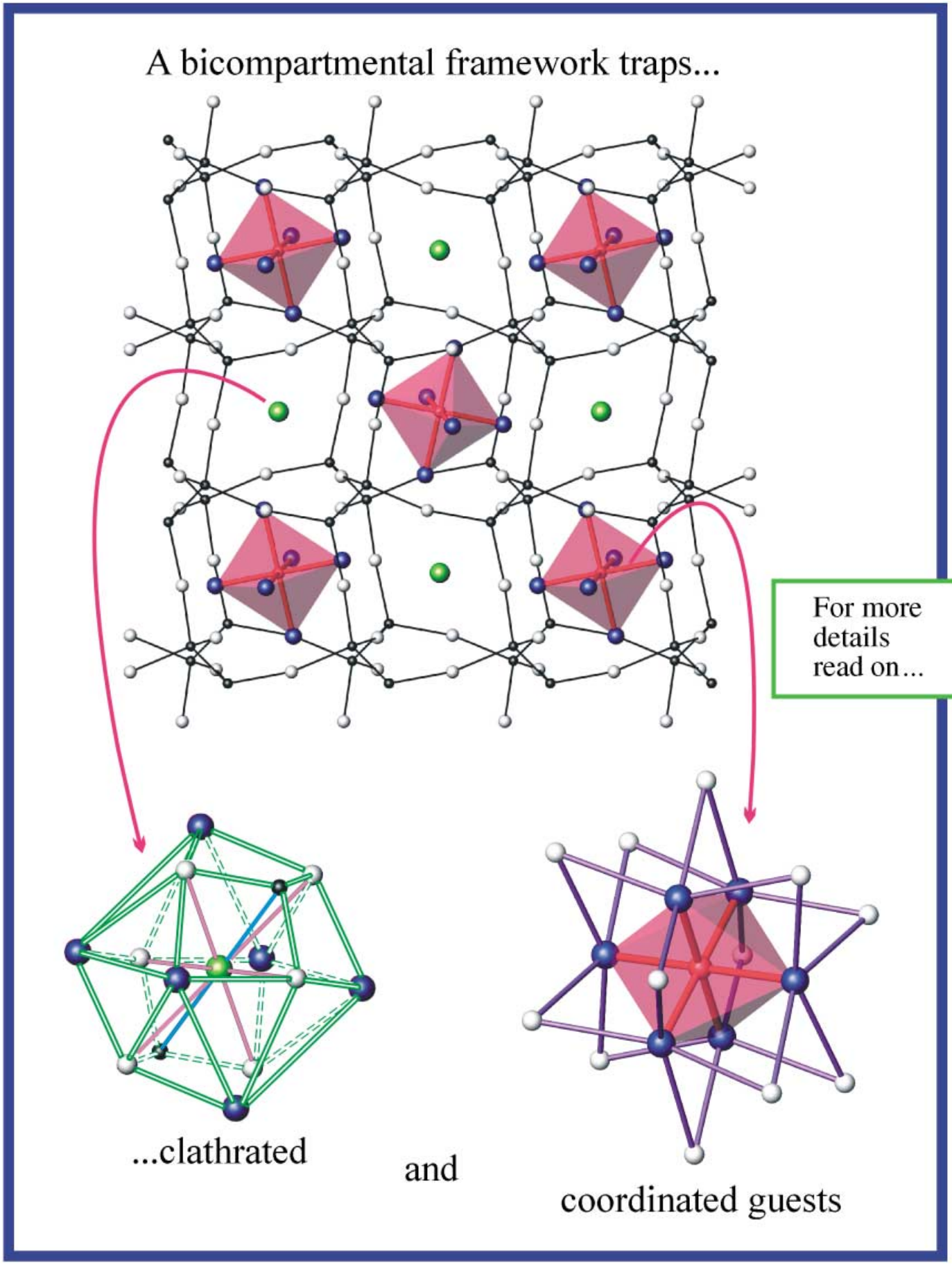

 DOI: 10.1002/chem.200204687

Coordinated and Clathrated Guests in the $_{\infty}^{3}[Hg_6As_4]^{4+}$ Bicompartmental Framework: Synthesis, Crystal and Electronic Structure, and Properties of the Novel Supramolecular Complexes $[Hg_6As_4](CrBr_6)Br$ and $[Hg_6As_4](FeBr_6)Hg_{0.6}$

Andrei V. Olenev,[b] Olga S. Oleneva,[b] Martin Lindsjö,[a] Lars A. Kloo,*[a] and Andrei V. Shevelkov*[b]

Abstract: Two new supramolecular complexes $[Hg_6As_4](CrBr_6)Br$ (**1**) and $[Hg_6As_4](FeBr_6)Hg_{0.6}$ (**2**) have been prepared by the standard ampoule technique and their crystal structures determined. Both crystallize in the cubic space group $Pa\bar{3}$ with the unit cell parameter $a = 12.275(1)$ (**1**) and 12.332(1) Å (**2**), and $Z = 4$. Their structures consist of bicompartmental, three-dimensional $[Hg_6As_4]^{4+}$ frameworks with cavities of two different sizes occupied by guest anions of different type. The bigger cavities are filled with the octahedral MBr_6^{n-} ions (M = Cr or Fe; $n = 3$ or 4), whereas the smaller cavities trap either Br^- ions (**1**) or Hg^0 (**2**). The analysis of the host–guest contacts has allowed a classification of the octahedral guests as coordinated and the monatomic guests as clathrated. Magnetic measurements and ESR spectroscopy data have given information about the interaction between the host and guests. Band structure calculations (HF and hybrid DFT level) indicate that both **1** and **2** are non-metallic, with a band gap of approximately 1.5 eV (B3LYP), and that the interaction between the host and guests is of predominantly electrostatic character. It is shown that though the electrostatic host–guest interaction is weak it plays an important role in assembling the perfectly ordered supramolecular architectures.

Keywords: arsenic · band structure · host–guest systems · mercury · solid-state structures · supramolecular chemistry

Introduction

The propensity of mercury to linear two-coordination can be exploited in the design of extended frameworks. In the well-known Millon's base salts,[1, 2] mercury together with four-coordinate nitrogen form cationic frameworks of the overall formula $[Hg_2N]^+$. Depending on the nature of the charge-compensating anions, the framework adopts either a tridymite[1] or a cristobalite[2] topology. The replacement of nitrogen by phosphorus gives rise to an $[Hg_2P]^+$ extended framework of the same topology, but containing bigger cavities. Now, larger anions, such as $HgBr_4^{2-}$[3] or ZnI_4^{2-},[4] are required to fill the cavities and provide electroneutrality.

Different mercury–pnicogen frameworks with other topological properties are also known.[5–9] Among them, those with a $[Hg_6Z_4]^{4+}$ framework,[6–9] in which Z = P, As or Sb, are of special interest for the following reasons: It is the only electrically charged Hg/Z extended framework that possesses cavities of two different sizes in close proximity. These are capable of trapping guests of two different types; octahedral guests in the bigger cavities and monoatomic guests in the smaller ones, showing a surprising difference in host–guest separation. Divalent[6] and trivalent[7–9] metal atoms are known to act as coordination centers for the octahedral guests, thus leaving the monoatomic guests to balance the charge.

Some attempts have been made to characterize the interactions between the host and the guests by means of calculations at the extended Hückel level.[5e, 9] Although the major part of the interaction is found to be electrostatic, some results indicate the possibility of a covalent contribution.[9] In any case, there is reason to make a more comprehensive analysis of the electronic structure.

[a] Prof. Dr. L. A. Kloo, M. Lindsjö
Inorganic Chemistry, Department of Chemistry
Royal Institute of Technology, Teknikringen 30
100 44 Stockholm (Sweden)
Fax: (+46) 8-790-9349
E-mail: larsa@inorg.kth.se

[b] Prof. Dr. A. V. Shevelkov, Dr. A. V. Olenev, O. S. Oleneva
Inorganic Synthesis Laboratory
Department of Chemistry
Moscow State University
Leninskie Gory 1/3
119992 Moscow (Russia)
Fax: (+7) 095-939-4788
E-mail: shev@inorg.chem.msu.ru

  DOI: 10.1002/chem.200204687

In the course of our research we have tried to use a series of the 3d metals from Cr to Ni as coordination centers for the octahedral guests, taking into consideration the ability of each of these metals to exhibit the formal oxidation states +2 and +3. Surprisingly, we succeeded only working with chromium and iron, for which two new compounds, $[Hg_6As_4](CrBr_6)Br$ (**1**) and $[Hg_6As_4](FeBr_6)Hg_{0.6}$ (**2**), were obtained. In this work we report the synthesis, crystal and electronic structure, as well as physical properties of the new phases, paying special attention to the inter-relationship of the host and guests and to the role of the different guests in stabilizing the supramolecular ensembles.

Results and Discussion

The crystal structure of one of the new phases is shown in Figure 1. The common feature of the structures is the $^3_\infty[Hg_6As_4]^{4+}$ framework. This framework is based on a four-connected As net with a γ-Si topology,[10] in which three of the

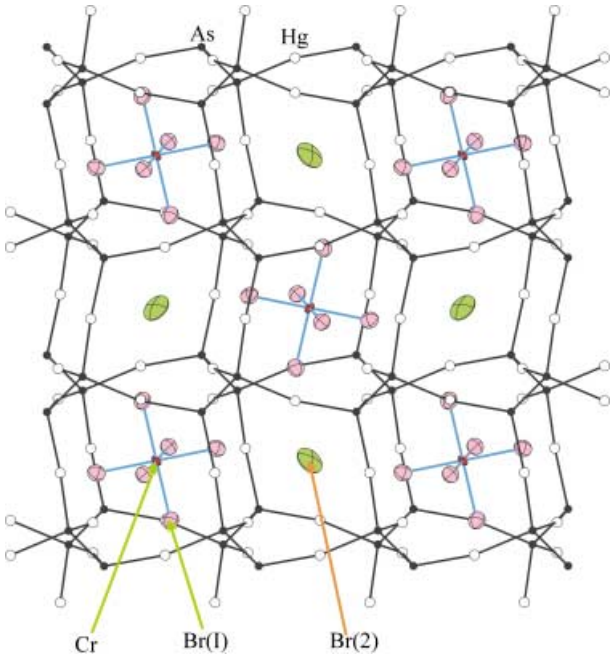

Figure 1. A slice of the crystal structure of $[Hg_6As_4](CrBr_6)Br$ showing the chess-board like ordering of two different guests, $CrBr_6^{3-}$ and Br^-, in the cavities of the $[Hg_6As_4]^{4+}$ framework. The guest anions are presented as 90% probability ellipsoids.

four edges are expanded[11] by Hg in such a way that the cubic symmetry is preserved (Figure 2). The As-Hg-As angle deviates slightly from linearity (165–167° in different structures) producing cavities of two different sizes, occurring in equal numbers and favoring an almost regular tetrahedral coordination of As. The As–As and As–Hg distances of 2.40–2.44 Å and 2.52–2.53 Å, respectively, are typical for various mercury arsenide halides.[5–8] The oxidation states of mercury and arsenic are quite apparent. The As–As separation is indicative of a single bond,[12] and therefore the As–As dumbbell can be regarded as an As_2^{4-} ion. Linearly coordi-

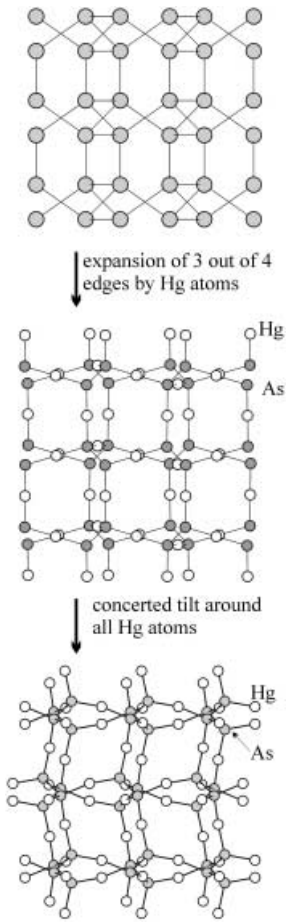

Figure 2. Hierarchy of the framework topology. Top: The structure of γ-Si, space group $Ia\bar{3}$. Middle: An idealized Hg_6As_4 framework, space group $Ia\bar{3}$. Bottom: The observed Hg_6As_4 framework, space group $Pa\bar{3}$. See text for explanation.

nated mercury, without Hg–Hg bonds, clearly has a +2 oxidation state. Consequently, the bicompartmental cationic framework can be formulated as $^3_\infty[Hg_6As_4]^{4+}$.

The guest anions should carry a total charge of −4 to compensate for the positive charge of the framework. In **1** this is achieved by a combination of two guest anions, $Cr^{III}Br_6^{3-}$ and Br^-, occupying the larger and smaller cavities, respectively. The same structural arrangement was previously found in several compounds that contain Ti^{3+} and Mo^{3+} as the centers of the octahedral guests.[7, 9] In **2**, the octahedral anions $Fe^{II}Br_6^{4-}$ do not require additional charge-compensating guests, whereas the smaller cavities trap excess mercury (with 60% occupancy). The partial occupancy of the smaller cavities by mercury atoms was previously observed in $[Hg_6As_4](HgCl_6)Hg_{0.4}$, whereby the zero valence of the excess mercury was confirmed by means of solid-state ^{199}Hg NMR spectroscopy.[13]

The M–Br distances within the octahedral guests differ from one compound to another. The Cr–Br separation of 2.52 Å is characteristic of Cr^{3+}, while the Fe–Br distance of 2.67 Å is typical for Fe^{2+}. Despite the difference in the M–Br bond length, both octahedral guests are almost of O_h symmetry; the deviation of the Br-M-Br angles from the octahedral ones do not exceed 2°, whereas the six M–Br

bonds are equidistant. Magnetic measurements and ESR spectra confirm the oxidation states of Cr and Fe. Complex **2** is diamagnetic, reflecting the t_{2g}^6 ground state of Fe^{2+}. A magnetic moment of 3.3 μ_B is found for **1**; this value is close to, though somewhat lower than, that predicted for Cr^{3+} (t_{2g}^3) by a spin-only model. The ESR spectrum of **1** shows a very broad signal, which is expected for Cr^{3+} in an O_h environment of six ligands.[14]

The host–guest distances in both phases are significantly longer than expected for covalent bonding; the feature being typical of supramolecular ensembles.[15] However, the coordination of the guest species is different. The separation between the Br(1) atom of the octahedral guest and Hg atoms of the framework ranges from 3.02 to 3.28 Å in **1** and **2**, being more than 0.5 Å longer than the Hg–Br covalent bond length, but is still in the bonding range. Each Hg atom has four distant bromine neighbors completing its coordination in a way similar to the coordination of Hg in $HgBr_2$. The 2+4 pseudo-octahedral array is achieved in the dibromide by two colinear bromine atoms in the first sphere, d(Hg–Br) = 2.48 Å, and four bromine atoms in the second sphere, d(Hg–Br) = 3.23 Å.[16] In **1** and **2** some distant Hg–Br(1) separations are even shorter (see Table 1) than those in

Table 1. Bond lengths [Å], valence angles [°], and nonbonding distances [Å] for **1** and **2**.[a]

	1	**2**
Hg(1)–As(1)	2.518(1)	2.524(1)
Hg(1)–As(2)	2.521(1)	2.528(1)
As(1)–As(2)	2.441(6)	2.422(6)
M–Br(1) × 6	2.519(3)	2.673(3)
As(1)-Hg(1)-As(2)	166.7(1)	165.65(1)
As(1)-As(2)-Hg(1) × 3	109.6(1)	110.95(9)
Hg(1)-As(2)-Hg(1) × 3	109.4(1)	107.9(1)
As(2)-As(1)-Hg(1) × 3	112.32(9)	107.1(1)
Hg(1)-As(1)-Hg(1) × 3	106.5(1)	111.73(9)
Br(1)-M-Br(1) × 3	180	180
Br(1)-M-Br(1) × 6	88.94(8)	87.99(8)
Br(1)-M-Br(1) × 6	91.06(8)	92.01(8)
Hg(1)–Br	3.182(1), 3.197(3)	3.046(2), 3.183(2)
	3.253(2), 3.349(2)	3.236(2), 3.285(2)
G–As(1) × 2	3.358(5)	3.548(4)
G–Hg(1) × 6	3.456(1)	3.700(1)
G–Br(1) × 6	3.805(3)	3.642(2)

[a] Labeling: M = Cr in **1**, Fe in **2**; G = Br(2) in **1** and Hg(2) in **2**.

$HgBr_2$. In this sense the octahedral anions are the **coordinated** guests. Indeed, the distant contacts "attach" the anions to their specific positions (Figure 3), and it is not surprising that no positional or rotational disorder is observed for them in this work, nor previously for the related phases.[6–9, 17]

The monatomic guests have a completely different environment. They display a coordination number of 14, with the host–guest separations falling in the range of 3.36–3.81 Å. With such a coordination, the monatomic guests can be regarded as **clathrated**. However, even the clathrated guests possess slightly different coordination depending on their nature (see Table 1 and Figure 4). When $Br(2)^-$ is a guest in **1**, two As and six Hg atoms are much closer to it than the six Br(1) atoms. In **2**, the 14 atom–atom distances from Hg(2) to

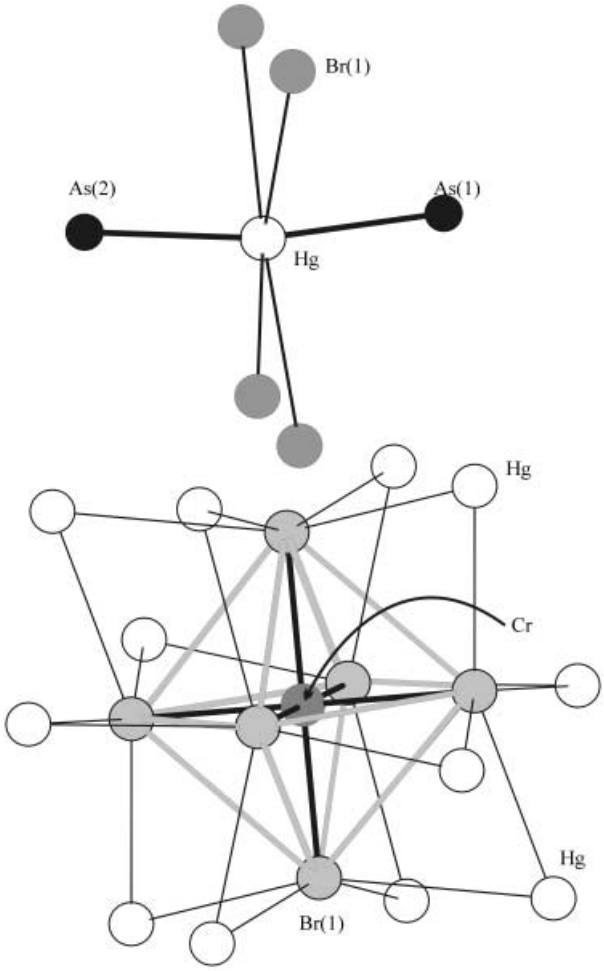

Figure 3. Coordination of Hg(1) (top) and environment of the octahedral guest (bottom) in **1**.

the ligands are distributed more uniformly; the six Hg(1) atoms being the most distant and beyond the Hg–Hg bonding limit.[18] Noticeably, the most distant neighbors are $Br(1)^-$ for $Br(2)^-$, and Hg(1) for Hg(2). It is reasonable to attribute this effect to the repulsive interactions, which must be the strongest between two closed-shell Br^- ions. Indeed, the Br(1)–Br(2) separation of 3.81 Å is the longest among all the host–guest distances.

The remaining question is why there are no analogues of the other transition metals? Any discussion about sizes of the octahedral guest can be discarded; the data shown in Table 1 clearly indicate that the M–Br distances can vary in the range of at least 2.52–2.67 Å, and small deviations from the regular octahedral shape are also allowed. However, as mentioned above, the octahedral guests should be considered as coordinated, and in return the geometry of the guest in the large cavity has to be octahedral to be able to coordinate to the host. Considering the fact that most octahedral coordination compounds of the first transition metal row are subjected to Jahn–Teller distortion from ideal octahedral symmetry, the number of potential guests are limited. Special cases are of course the d^0 and d^{10} systems. Considering the low-spin case, only the configuration t_{2g}^6 is expected to give suitable guests (Fe^{2+}, Co^{3+}). In the case of the mercury–arsenide framework,

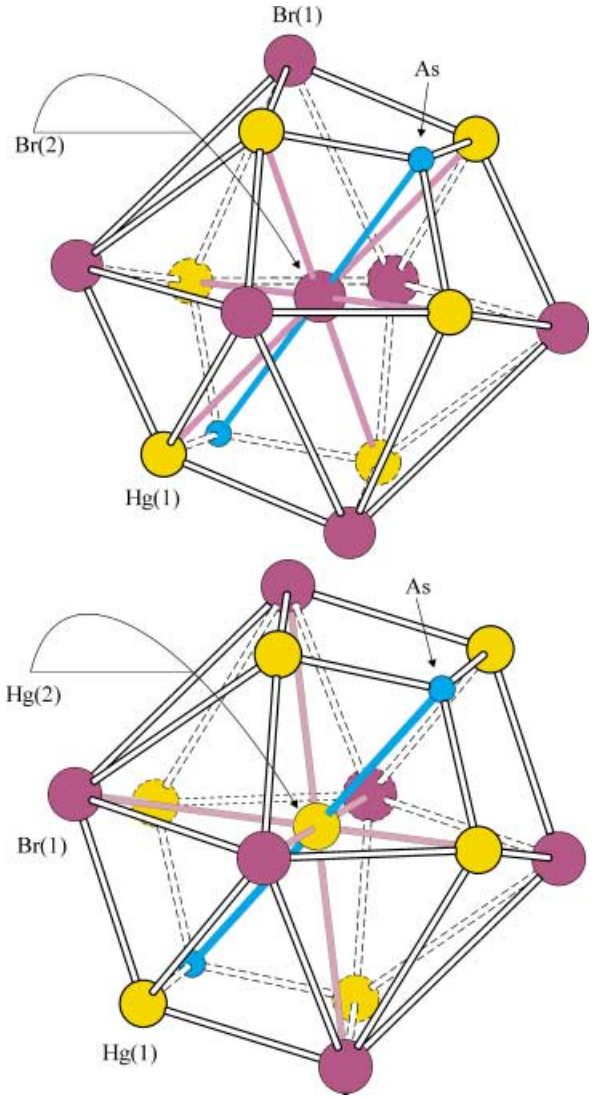

Figure 4. Coordination of the monoatomic (clathrated) guest. Top: Br(2) in **1**; Bottom: Hg(2) in **2**. Eight less distant host–guest contacts are indicated with bold lines in each case.

the oxidative power of Co^{3+} ions is expected to be too high with respect to the arsenide framework, and therefore the compound $[Hg_6As_4](CoBr_6)Br$ is less likely to be formed. For the high-spin case, there are more options: t_{2g}^3 (V^{2+}, Cr^{3+}), $t_{2g}^3e^{*2}_g$ (Mn^{2+}, Fe^{3+}), and $t_{2g}^6e^{*2}_g$ (Ni^{2+}), although the last two options demand unfavorable occupation of the e^*_g level. It is evident that almost all of the possibilities for which the e^*_g level is unoccupied are exhausted. Anyhow, there is a motive to investigate the bonding scheme, in particular the interaction between the host framework and the guest moieties. For this purpose, we performed band structure calculations for both $[Hg_6As_4](CrBr_6)Br$ and a hypothetic $[Hg_6As_4](FeBr_6)$ complex, which is similar to **2** but with the smaller cavities left empty.

Special care has to be taken to obtain correct results when calculating the electronic structure for compounds that contain transition elements, because of the partially filled d orbitals, in particular those with unpaired d electrons. In the case of $[Hg_6As_4](FeBr_6)$ there are two possible d electron configurations, adapting a crystal field theory view: low-spin (t_{2g}^6) or high-spin ($t_{2g}^4e^{*2}_g$). However, the high-spin configuration is expected to be distorted, due to Jahn–Teller effects. Since the structural data show no effects of this kind and, instead, an almost perfect octahedral structure is observed, we assume the configuration to be low-spin. This is also confirmed by the magnetic susceptibility measurements. Also, the theoretical calculations indicate this to be the most stable solution. Nevertheless, for a final conclusion in this matter accurate magnetic and Mössbauer spectroscopy measurements down to low temperatures have to be performed.

Measurements show that large crystals of **1** and **2** exhibit a resistivity of several kΩ at room temperature. Looking at the density of states (DOS) plot for (pseudo-)**2**, t_{2g}^6-$[Hg_6As_4](FeBr_6)$, at the B3LYP level (Figure 5), the band

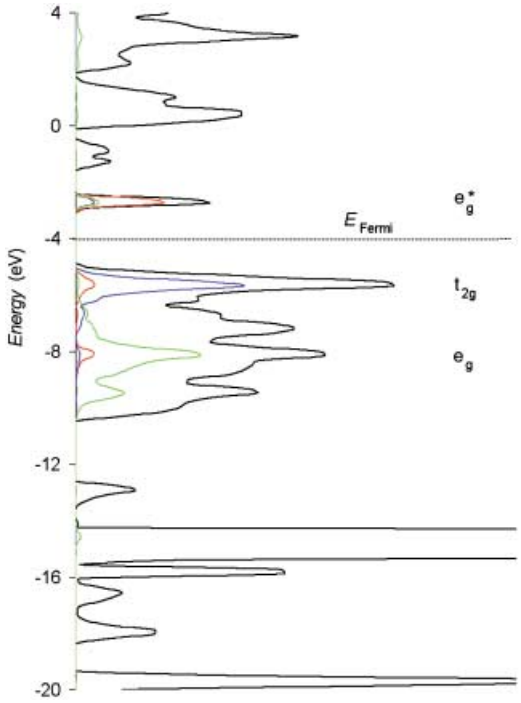

Figure 5. The DOS plot for pseudo-**2** $[Hg_6As_4](FeBr_6)$ at B3LYP level of theory. Total: black; Fe: d_{xy}, d_{xz}, d_{yz} (t_{2g}) orbitals blue; Fe: d_{z^2}, $d_{x^2-y^2}$ (e_g) orbitals red; Br: p_z (σ-type orbitals) green.

gap is found to be 1.8 eV (the UHF results are in general agreement), and a nonmetallic behavior is to be expected. The most noticeable feature of the DOS is that the d orbitals of the iron atoms, the central atoms of the octahedral guests, form very narrow bands, hence indicating localized orbitals. In fact, the bonding situation of the $FeBr_6^{4-}$ guest is fully understood on a simple ligand-field theoretical level. Thus, the conduction band consists entirely of contributions from the $FeBr_6^{4-}$ guest; for example, the anti-bonding e^*_g orbitals of the $FeBr_6^{4-}$ octahedron. The t_{2g} band of the octahedral guest is found at the top of the valence band, localized to the iron atoms as expected from their nonbonding character. In contrast, the e_g band, which is found well below the Fermi level, is almost completely localized to the bromine atoms. Calculations were also performed for the other extreme composition, $[Hg_6As_4]$-$(FeBr_6)Hg$, with the mercury atoms in all of the smaller

cavities. The results were analogous to those of the $[Hg_6As_4]$-$(FeBr_6)$ composition. However, a small contribution from the clathrated mercury atoms appears at the top of the valence band.

In the case of $[Hg_6As_4](CrBr_6)Br$ (**1**), the results are somewhat more complicated owing to the three (experimentally verified) unpaired d electrons of chromium. The populations of electrons in α and β spin states now differ, and, therefore, the DOS has to be separated into two spin-dependent plots (Figure 6). Still, the appearance of the β-spin

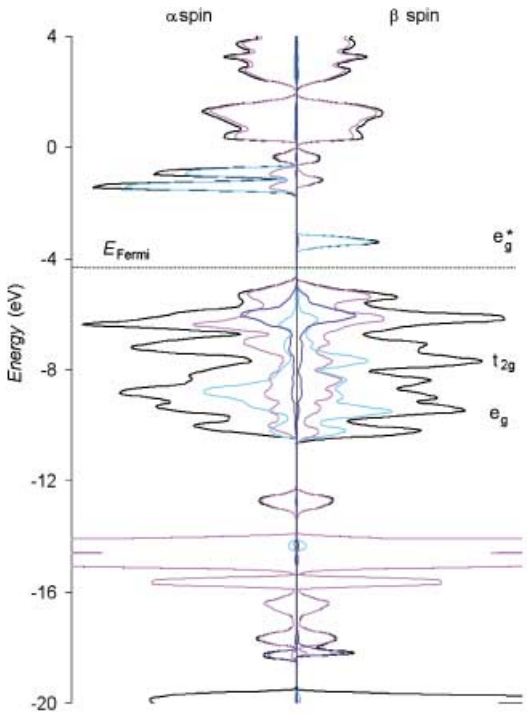

Figure 6. The DOS plot for **1** at B3LYP level of theory. Total, black; Host: pink; octahedral guest: σ-type orbitals (Cr: d_{xy} d_{xz}, d_{yz}, d_{z^2}, $d_{x^2-y^2}$ and Br: p_z) light blue; bromine guest: dark blue.

DOS is quite similar to the DOS of **2**; the conduction band is entirely consisting of the e^*_g orbitals of the octahedral guest, and in the valence band both the t_{2g} and e_g bands can be found. However, as the octahedral bands are shifted in energy relative to the host when changing the central atom of the guest, the band gap has decreased to 1.0 eV, and the t_{2g} band has moved down in the valence band. Also the clathrated bromide guest forms narrow bands. The narrow guest bands, as well as the fact that the ligand-field theory can predict the electronic structure of the octahedral guests so successfully, are indications that electrostatic interactions between host and guests predominate. Also, the DOS plots suggest that the band gap in these materials is dependent on the energy of the e^*_g molecular orbitals of the octahedral guest.

Plots of the electron density difference and particularly the electron localization function (ELF) are very useful for observing any covalent interactions between atoms,[19] and for the two compounds studied in this work special interest is focused to the interaction between host and guests. In neither **1** or **2** any such interaction can be directly observed. This confirms that the host–guest interactions are of predominantly electrostatic nature.

Mulliken populations could also provide some information about the bonding, especially those of the guests. In this study some charge transfer can be observed from the guests to the host, but this most likely only reflects an expansion of the guest valence orbitals in the closed cavity. Because of the diffuse nature of this expansion, no specific interactions can be detected between the guests and the host by using plots of the electron density difference or ELF.

The overall results indicate that the host–guest interaction plays an important role in stabilizing the solid-state, supramolecular complexes, but that the nature of these interactions is diffuse and weak; no significant covalent interaction appears to be present. Moreover, we are convinced that these weak interactions are important in assembling the architectures from intermediates that are formed in the course of the high-temperature ampoule synthesis, similar to the designed self-assembling of bi- and multicompartmental ensembles from complex mixtures in solutions at about room temperature.[20] This approach has also pointed out the possibility in forming supramolecular complexes that include fragments not attainable in solution, for example, $FeBr_6^{4-}$.

In the new phases **1** and **2**, the two different guests are encapsulated in closed cavities of the host framework. Evidently, the guests cannot enter or leave their specific cavities, nor can the electrically charged framework exist without the encapsulated charge-compensating guests. Consequently, they can form only spontaneously through a self-process, in which the host and guests form simultaneously and the guests serve as templates supporting the formation of the framework. The perfect ordering of the guests in the cavities of the framework indicates that such a process includes chemical recognition,[21] according to which the guest of a certain type, coordinated or clathrated, positions itself in the proper cavity.

Experimental Section

Synthesis: The following starting materials were used: liquid mercury, gray arsenic, chromium powder, and iron powder, all of high purity (= 99.995 %). Mercury(I) bromide was prepared by a reaction of excess mercury(I) nitrate with potassium bromide in aqueous solution, followed by drying of a precipitate in vacuum at room temperature. Mercury(II) bromide was synthesized by direct reaction of liquid mercury and excess bromine at ambient temperature. The product was re-crystallized from ethanol, washed with water and acetone, and then vacuum-dried. Mercury bromides as well as elemental arsenic were checked before use by X-ray powder analysis [STADI-P (STOE), Cu-$K_{\alpha 1}$ radiation]. The syntheses were carried out using a standard ampoule technique. Details are given below.

Compound 1: A stoichiometric mixture of Hg_2Br_2, $HgBr_2$, As, and Cr (1 g total weight) was sealed in a silica tube, annealed at 780 K for 4 days, and furnace-cooled. The dark-violet air-stable product contained no X-ray detectable impurities. All lines on a Guinier photograph (Nonius FR-552 chamber, $Cu_{K\alpha 1}$ radiation) were indexed in a cubic system with a = 12.264(1) Å. For the single-crystal preparation, a mixture of Hg_2Br_2, As, and Cr taken in a 3:4:1 molar ratio was annealed in a silica tube for 5 days at 780 K. Dark violet crystals with a cubic shape were found in the furnace-cooled product.

Compound 2: A stoichiometric mixture of Hg_2Br_2, Hg, As, and Fe (1 g total weight) was annealed in a vacuum-sealed silica tube at 670 K for 4 days. An X-ray analysis of a black, air-stable product showed no traces of impurities. All lines on a Guinier photograph were indexed in a cubic cell by analogy with **1**. For the single-crystal preparation, a mixture of the same starting materials in a 3:1:4:1 molar ratio was annealed in a silica tube at 650 K for 5 days. Black single crystals with a cubic shape were found in the furnace-cooled product. A crop of crystals was selected for chemical analysis (SGAB Analytica, Luleå, Sweden), which showed the Hg:Fe molar ratio to be 6.59:1; this is in excellent agreement with the synthetic and structural data.

Crystal structure determination: The crystal structures of **1** and **2** were determined based on single-crystal X-ray experiments. For this, suitable crystals were mounted on a CAD4 (Nonius) goniometer head. The cubic unit cell parameters (Table 2) were refined based on 24 well-centered reflections in the angular range $11^\circ < \theta < 14^\circ$. The data sets were collected in an $\omega/2\theta$ mode. Semiempirical absorption corrections were applied to both data sets based on ψ-scans of several reflections with χ angles close to 90°. Systematic absences pointed to the space group $Pa\bar{3}$ (No. 205) for all structures. In all cases the SHELXS-97 and SHELXL-97 programs[22] were used for the structure solution and refinement, respectively. Crystallographic data for **1** and **2** are listed in Table 2; atomic parameters are listed in Table 3, and bond distances and angles, and important nonbonding distances are collected in Table 1. Details of the crystal structure refinement relevant to each structure are given below.

Table 2. Crystallographic data for **1** and **2**.

	1	**2**
formula	$[Hg_6As_4](CrBr_6)Br$	$[Hg_6As_4](FeBr_6)Hg_{0.59(1)}$
M_r	2114.59	2157.38
a [Å]	12.275(1)	12.332(1)
V [Å]	1849.5(3)	1875.4(3)
space group	$Pa\bar{3}$	$Pa\bar{3}$
Z	4	4
T [K]	292	292
λ [Å]	0.71069	0.71069
ρ_{calcd} [g cm^{-3}]	7.594	7.641
μ [cm^{-1}]	723.77	742.26
$R(F_o)$[a]	0.0632	0.0538
$R_w(F_o^2)$[b]	0.1178	0.1062

[a] $R(F_o) = \Sigma ||F_o| - |F_c|| / \Sigma |F_o|$. [b] $R_w(F_o^2) = [\Sigma w(F_o^2 - F_c^2)^2 / \Sigma w(F_o^2)^2]^{1/2}$, $w = [\sigma^2(F_o^2) + 0.0310(F_o^2 + 2F_c^2)/3]^{-1}$.

*Compound **1***: Positions of all atoms were found from direct methods. Final anisotropic refinement against F^2 led to $R_1 = 0.0632$.

Table 3. Atomic coordinates and equivalent thermal displacement parameters for **1** and **2**.

Atom	Wyckoff	x/a	y/b	z/c	U_{eq} [10^{-3} Å^2][a]
Compound **1**					
Hg(1)	*24d*	0.2994(1)	0.4604(1)	0.1936(1)	19(1)
As(1)	*8c*	0.1579(2)	0.1579(2)	0.1579(2)	9(1)
As(2)	*8c*	0.2727(2)	0.2727(2)	0.2727(2)	9(1)
Cr	*4b*	0	0	1/2	4(2)
Br(1)	*24d*	0.0402(2)	0.4544(2)	0.1960(2)	14(1)
Br(2)	*4a*	0	0	0	30(2)
Compound **2**					
Hg(1)	*24d*	0.2858(1)	0.4717(1)	0.2082(1)	13(1)
As(1)	*8c*	0.1661(2)	0.1661(2)	0.1661(2)	4(1)
As(2)	*8c*	0.2795(2)	0.2795(2)	0.2795(2)	6(1)
Fe	*4b*	0	0	1/2	5(2)
Br(1)	*24d*	0.0390(2)	0.4618(2)	0.2097(2)	12(1)
Hg(2)	*4a*	0	0	0	38(2)

[a] U_{eq} is defined as one third of the trace of the orthogonalized U_{ij} tensor.

*Compound **2***: Positions of all atoms were found from direct methods. The atom at the *4a* position was refined isotropicaly as mercury having 60.0(8) % occupancy. Attempts to refine it as 100 % occupied by bromine led to an abnormally low (zero) thermal displacement parameter and to contradiction with the overall charge balance, since it would imply a +3 oxidation number of iron and a paramagnetic behavior that was not observed (vide infra). Final anisotropic refinement against F^2 led to $R_1 = 0.0538$ and to the overall composition $Hg_{6.59(1)}As_4FeBr_6$ that was in excellent agreement with the chemical analysis.

Further details of the crystal structure determination may be obtained from Fachinformationszentrum Karlsruhe, D-76344 Eggenstein-Leopoldshafen, Germany, on quoting the depository numbers CSD-411481 (**1**) and 411483 (**2**).

Magnetic susceptibility measurements: Magnetic susceptibility measurements were performed on **1** and **2** by using a standard Faraday balance technique. Before use, the purity of the samples was checked by means of a profile analysis of the respective X-ray powder diffractogram [STADI-P (STOE), $Cu_{K\alpha 1}$ radiation]. After correction for the Langevin term, a magnetic moment of 3.3(1) μ_B was obtained for **1**. **2** was found to be diamagnetic.

ESR spectroscopy: The ESR spectrum of **1** was recorded on EMX 1104 (Bruker) spectrometer operated at 9.5 GHz. The purity of the finely powdered sample was checked as described above.

Band structure calculations: These were performed with the CRYSTAL98 program package.[23] All calculations included converged SCF with unrestricted spin, and evaluation of band structure and density of states (DOS), at both Hartree–Fock (HF) and hybrid density functional theory level (B3LYP). For chromium and iron, all-electron basis sets (8s12sp5d)/{86–41141G}, available on the CRYSTAL website, were used.[24] For the remaining atom types, Hay and Wadt large-core (HAYWLC) pseudopotentials[25] were applied as implemented in CRYSTAL98, except for mercury for which f-potentials had to be excluded due to restrictions of the program (this is a limited problem since f-functions were not used in the valence basis sets). The corresponding valence basis sets by Hay and Wadt, with double-zeta quality, were used with some modifications; the most diffuse functions of the metals were removed in order to minimize convergence problems, and the other functions were decontracted.

Electron density maps and electron localization function (ELF)[19] were calculated using TOPOND 98.[26]

Acknowledgement

This work was supported by Russian Foundation for Basic Research, grant 00–03–32539a, and by INTAS, Contract No. 99–01672 and RTN # HPRN-CT-2002–00193.

[1] a) L. Nijssen, W. N. Lipscomb, *Acta Crystallogr.* **1954**, *7*, 103–106; b) W. Rüdorff, K. Brodersen, *Z. Anorg. Allg. Chem.* **1953**, *274*, 323–340.
[2] R. Airoldi, G. Magnano, *Rass. Chim.* **1967**, *5*, 181–189.
[3] A. V. Shevelkov, M. Y. Mustiakimov, E. V. Dikarev, B. A. Popovkin, *J. Chem. Soc. Dalton Trans.* **1996**, *1*, 147–148.
[4] A. V. Olenev, A. V. Shevelkov, B. A. Popovkin, *Zh. Neorg. Khim.* **1999**, *44*, 1911–1913.
[5] a) H. Puff, M. Grönke, B. Kilger, P. Möltgen, *Z. Anorg. Allg. Chem.* **1984**, *518*, 120–128; b) A. V. Olenev, A. V. Shevelkov, B. A. Popovkin, *Zh. Neorg. Khim.* **1999**, *44*, 1957–1965; c) A. V. Olenev, A. I. Baranov, A. V. Shevelkov, B. A. Popovkin, *Eur. J. Inorg. Chem.* **2000**, 265–270; d) A. V. Olenev, A. V. Shevelkov, *Angew. Chem.* **2001**, *113*, 2415–2416; *Angew. Chem. Int. Ed.* **2001**, *40*, 2353–2354; e) J. Beck, U. Neisel *Z. Anorg. Allg. Chem.* **2001**, *627*, 2016–2022; f) A. V. Olenev, A. I. Baranov, A. V. Shevelkov, B. A. Popovkin, *Eur. J. Inorg. Chem.* **2002**, 547–553.
[6] A. V. Shevelkov, E. V. Dikarev, B. A. Popovkin, *J. Solid State Chem.* **1996**, *126*, 324–327.
[7] J. Beck, U. Neisel, *Z. Anorg. Allg. Chem.* **2000**, *626*, 1620–1626.
[8] a) J. Beck, S. Heddereich, U. Neisel, *J. Solid State Chem.* **2000**, *154*, 350–355; b) A. V. Olenev, M. M. Shatruk, A. V. Shevelkov, B. A.

Popovkin. *Zh. Neorg. Khim.* **2002**, *46*, 1615 – 1618; c) A. V. Olenev, A. I. Baranov, M. M. Shatruk, A. S. Tyablikov, A. V. Shevelkov. *Izv. Akad. Nauk. Ser. Khim.* **2002**, N3, 414 – 418; e) *Russ. Chem. Bull.* **2002**, *51*, 444 – 448.
[9] A. V. Olenev, A. V. Shevelkov, *J. Solid State Chem.* **2001**, *160*, 88 – 92.
[10] J. S. Kasper, S. M. Richards, *Acta Crystallogr.* **1964**, *17*, 752 – 755.
[11] M. O'Keefe, M. Eddaoudi, H. Li, T. Reineke, O. M. Yaghi, *J. Solid State Chem.* **2000**, *152*, 3 – 20.
[12] H. G. von Schnering, *Angew. Chem.* **1981**, 93, 44 – 62; Angew. *Chem. Int. Ed. Engl.* **1981**, *20*, 33 – 51.
[13] A. V. Shevelkov, *Book of Abstracts*, *6th European Conference on Solid State Chemistry*, Zürich, Switzerland, **1997**, Abstract ML7.
[14] For the theoretical background and examples, see R. S. Drago, *Physical Methods in Chemistry*, Saunders, **1977**, Chapter 13.
[15] A. Müller, H. Reuter, S. Dillinger, *Angew. Chem.* **1995**, *107*, 2505 – 2539; *Angew. Chem. Int. Ed. Engl.* **1995**, *34*, 2328 – 2361.
[16] V. I. Pakhomov, A. V. Goryunov, I. N. Ivanova-Korfini, A. A. Boguslavskii, R. S. Lotfullin, *Zh. Neorg. Khim.* **1990**, *35*, 2476 – 2478.
[17] A. V. Shevelkov, L. N. Reshetova, B. A. Popovkin, *J. Solid State Chem.* **1998**, *137*, 138 – 142.
[18] a) P. Pyykkö, *Chem. Rev.* **1997**, *97*, 597 – 636; b) A. V. Shevelkov, M. M. Shatruk, *Izv. Akad. Nauk. Ser. Khim.* **2001**, 321 – 335; *Russ. Chem. Bull. Int. Ed.* **2001**, *50*, 337 – 352. and references therein
[19] A. D Becke, K. E. Edgecombe, *J. Chem. Phys.* **1990**, *92*, 5397 – 5403.
[20] a) P. N. W. Baxter, J.-M. Lehn, G. Bahn, D. Fenske, *Chem. Eur. J.* **2000**, *6*, 102 – 112; b) P. N. W. Baxter, J.-M. Lehn, G. Bahn, B. O. Kneisel, D. Fenske, *Chem. Eur. J.* **1999**, *5*, 113 – 120; c) A. Müller, V. P. Fedin, E. Diemann, H. Bögge, E. Krickemeyer, D. Sölter, A. M. Giuliani, R. Barbieri, P. Adler, *Inorg. Chem.* **1994**, *33*, 2243 – 2245.
[21] J.-M. Lehn, *Supramolecular Chemistry*, VCH, Weinheim, **1995**.
[22] a) G. M. Sheldrik, SHELXS-97, program for crystal structure solution, University of Göttingen (Germany) **1997**; b) G. M. Sheldrik, SHELXL-97, program for crystal structure refinement, University of Göttingen, (Germany), **1997**.
[23] a) " HF ab-initio Treatment of Crystalline Systems":C. Pisani, R. Dovesi, C. Roetti, *Lecture notes in Chemistry*, *Vol. 48* Springer, Berlin, **1988**; b) V. R. Saunders, R. Dovesi, C. Roetti, M. Causà, N. M. Harrison, R. Orlando, C. M. Zicovich-Wilson, *CRYSTAL98*, University of Torino, Torino, **1998**.
[24] M. D. Taylor, **1992**, to be found under www.chimifm.unito.it/teorica/crystal/Basis Sets/mendel.html
[25] a) P. J. Hay, W. R. Wadt, *J. Chem. Phys.* **1985**, *82*, 270 – 283; b) P. J. Hay, W. R. Wadt, *J. Chem. Phys.* **1985**, *82*, 284 – 298.
[26] C. Gatti, Topond 98 User's Manual, CNR-CSRSRC, Milano, **1999**.

Received: December 19, 2002 [F4687]

